CHEMIJA. 2022. Vol. 33. No. 4. P. 111–119

A novel strategy to develop electrochemical atrazine sensor

Emilija Katinaitė[1],

Vytautas Žutautas,

Aneta Bytautaitė,

Rasa Pauliukaitė*

Department of Nanoengineering,
Center for Physical Sciences and Technology,
231 Savanorių Avenue,
02300 Vilnius, Lithuania

[1] Present address:
UAB Thermo Fisher Scientific Baltics,
8 Graičiūno Street,
02241 Vilnius, Lithuania

Determination of pesticides is important for human health. Sensors are one of the best solutions because they do not require a long sample preparation and can be used not only in a laboratory. Electrochemical sensors can be easily minimised and employed for the detection of pesticides in liquid samples such as ground or wastewater. Conducting polymers have a few roles in electrochemical sensors, therefore, they can be good candidates for sensor development. Electrochemically co-polymerised folic acid and riboflavin as well as folic acid and L-lysine were employed for the detection of atrazine using square wave voltammetry. The co-polymer composition was optimised and characterised electrochemically and spectroscopically. The optimal composition of polyfolic acid and poly-L-lysine co-polymer electrosynthesised from the monomer ratio 1:10 was the best in terms of stability and sensitivity to atrazine. The best method was the square wave voltammetry showing the best sensitivity to atrazine 198 ± 1 μA/μM cm^2, and the limit of detection was 14.8 nM. However, the sensitivity in tap water was significantly lower but still suitable for atrazine detection by the spike method.

Keywords: electrochemical sensor, atrazine, co-polymer, riboflavin, folic acid, L-lysine

INTRODUCTION

In agriculture, it is hardly possible to have a good crop productivity without the prevention from various plant parasites including microorganisms, weeds or small animals. To increase crop yield and its resistivity to diseases, agriculturers use pesticides, one kind of which are herbicides. However, herbicides are toxic to the same plants in high concentrations, moreover, especially toxic to animals and humans. Many of the older and cheaper pesticides contain an organochlorine group which can remain for years in soil and water and can accumulate in the food chain. These chemicals have been banned by countries that signed the 2001 Stockholm Convention [1]. However, some of them might be still left in an ecosystem. Therefore, there is a high demand to monitor their concentrations in drinking water and soil. Moreover, some agriculturers are abusing the consumption of pesticides on all continents [1].

Atrazine or diamino-1,3,5-triazine is one of the most toxic organochlorine group compounds found in groundwater. Its chemical structure is given in Fig. 1. Moreover, due to its low solubility in water, it can be found also in the food chain [2].

Usually, atrazine is determined with chromatographic methods [3–6]. Also, other methods are being developed such as spectroscopic [7–9] and electrochemical [10–17]. Electrochemical determination in most cases is performed via

* Corresponding author. Email: rasa.pauliukaite@ftmc.lt

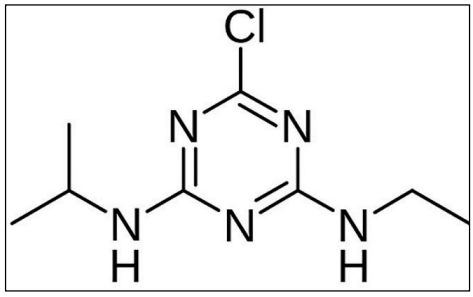

Fig. 1. Chemical structure of diamino-1,3,5-triazine

electrochemical sensors [10, 13, 16–19] and immunosensors [11, 12, 14, 20] based on various composites and nanoparticles. The large group of electrochemical (bio)sensors is based on conducting polymers such as polyaniline and imprinted polymers or their composites with nanomaterials [21–23].

Although a number of sensing approaches have been published, the majority of them require expensive materials and complex construction. Polymers composed of vitamin B group compounds have been already successfully applied for sensing applications [24–26]. Owing to this, it is a novel approach to test these polymers for the determination of atrazine.

In this work, co-polymers of riboflavin (Rf, vit. B2), folic acid (FA, vit. B9) and L-lysine (LL) were applied to develop a sensor for atrazine. The polymerisation, microscopic and electrochemical characterisation of the obtained co-polymers, and electrochemical detection of atrazine were studied.

EXPERIMENTAL

Folic acid and riboflavin were from Alfa Aesar (USA), L-lysine, KCl, K_2SO_4, $K_4[Fe(CN)_6]\cdot 3H_2O$, NaH_2PO_4, Na_2HPO_4 and HCl were from Sigma Aldrich (Germany). NaOH and NaCl were obtained from ROTH GmbH (Germany). All used reagents were of analytical grade and used as received.

Aqueous solutions were prepared in the ultrapure MilliQ-water (resistivity of 18.2 MWcm) taken from a Synergy 185 unit with a UV lamp (Millipore, USA).

For electrochemical experiments, 0.1 M sodium phosphate buffer saline with 0.15 M NaCl (PBS), pH 5.00 ± 0.04, 5.50 ± 0.03 and 6.00 ± 0.04, was used as a supporting electrolyte. In some cases, the supporting electrolyte was 0.1 M KCl with the addition of 0.01 M HCl, pH 2.00 ± 0.04.

The 3-electrode cell is used for electrochemical measurements, where Pt wire served as a counter electrode and Ag/AgCl with sat. KCl solution was used as a reference (all data are given vs this electrode). All measurements were performed with a potentiostat/galvanostat CompactStat (Ivium Technologies, the Netherlands). A glassy carbon electrode (GCE) with a diameter of 3 mm was used as a working electrode. Prior to electrode modification, it was cleaned mechanically using Al_2O_3 nanoparticles of 1.0 μm, 0.30 μm and 0.05 μm on a micropolishing pad for 5–8 min. After each polishing step one particle size, the electrode is rinsed with MiliQ water and sonicated in MiliQ water and ethanol for 10 s in each step. The next step is electrochemical polishing in 0.1 M KCl solution, in the cyclic voltammetry (CV) mode at the potential scan rate of 100 mV/s, within the potential range from –1.00 V to +1.00 V until the steady state is reached. Finally, the electrode is rinsed with the MiliQ water and dried under a N_2 stream.

Highly oriented pyrolytic graphite (HOPG, NTMTD, Ireland) was used for microscopic investigations instead of GCE. Prior to modification, the electrode surface was cleaved with an adhesive tape and immediately coated with a copolymer.

Square wave voltammetry (SWV) was performed for atrazine detection adding aliquots of the analyte to 0.1 M PBS, pH 5.0. SWV parameters were the following: the pulse frequency 50 Hz, the potential pulse amplitude 10 mV.

Chronoamperometry was performed at an optimised potential of –0.6 V vs Ag/AgCl (sat. KCl) in the same solution as in the case of SWV.

Atomic force microscopy (AFM) was performed using a Nano Wizard3 (JPK, Germany). The surface imaging was carried out in the air at room temperature. The PPP-XYNCSTR AFM tip (Nanosensors) was used, and the images were registered using a vibrating mode.

Co-polymers were prepared by electrochemical polymerisation of monomers at freshly prepared GCE. Polymerisation conditions are given in Table 1. After the polymerisation, the electrodes were left for 1 day in air to cure. Afterwards, the electrodes were characterised electrochemically or employed for atrazine detection.

When HOPG was used as an electrode substrate, 150 μL of the electropolymerisation solution was dropped on the surface. Then, a micro Pt-wire

counter electrode and a micro Ag/AgCl reference electrode were inserted into the droplet and co-polymer was synthesised applying the same procedure as in the case of GCE just for 10 cycles.

RESULTS AND DISCUSSION

Since it was known from our previous works that poly(folic acid) (PFA) and polyriboflavin (PRf) act as mediators in electrochemical sensing [24–26], they were chosen to modify the electrode with a sensitive layer. Figure 2a, b represent the electropolymerisation of FA and Rf, respectively. It was found in the previous works that PFA assures better sensitivity to an analyte but PRf guarantees better stability of a biosensor [24, 25]. Therefore, a co-polymer PFA-PRf was synthesised on the GCE surface (Fig. 2c, d) in this study. In order to optimise polymerisation conditions, different FA and Rf ratios were chosen to obtain a co-polymer with the best electroanalytical properties. Three compositions were used as indicated in Table 1.

The polymerisation CV profiles for PFA-PRf3 and PFA-PRf5 were identical, therefore, only one polymerisation CV set is indicated in Fig. 1c. As seen, the polymerisation CV differs from both FA and Rf separately. However, peak numbers and positions are more similar to FA polymerisation rather than to Rf. In the co-polymer, the formation of radicals is better expressed at ca. +0.90 V (Fig. 2c, d).

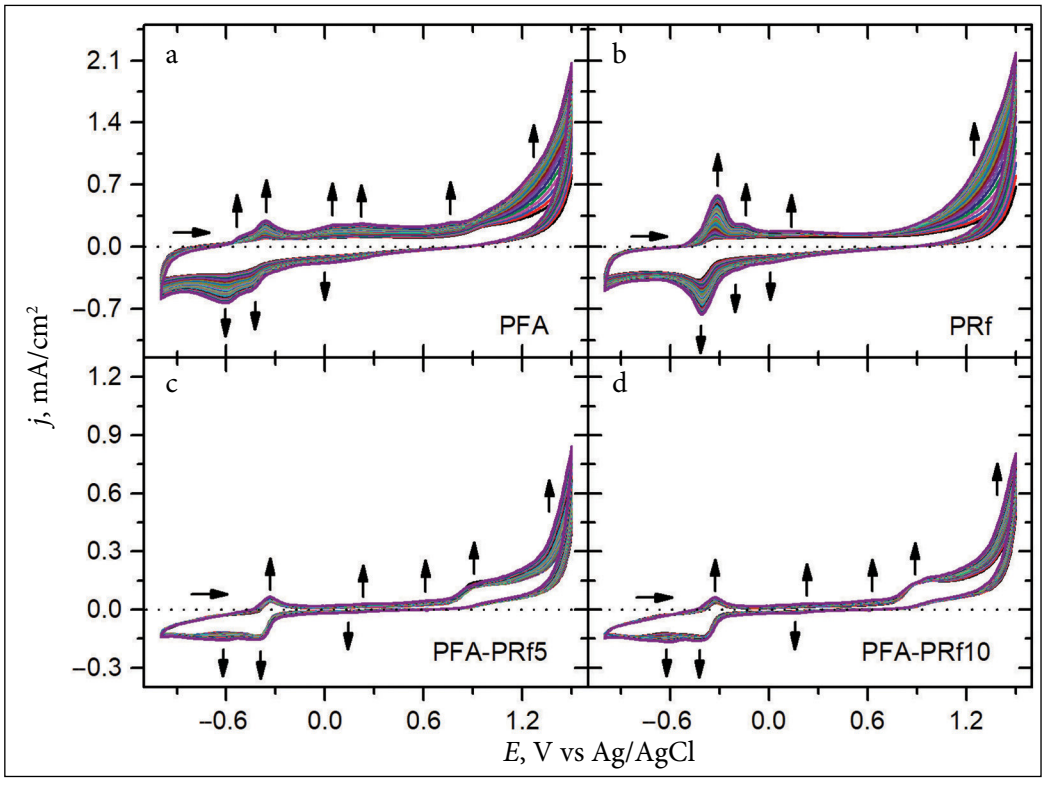

Fig. 2. CVs of the electropolymerisation of 1.0 mM FA at GCE in 0.1 M PBS, pH 5.0 (a), 10.0 mM Rf at GCE in 0.1 M PBS, pH 7.0 (b), FA-Rf, monomer ratio was 1:5 (c) and 1:10 (d) at GCE in 0.1 M PBS, pH 6.0. The potential interval between −1.0 V and +1.5 V, number of cycles 32, scan rate 50 mV/s. Vertical arrows show changes in the current with the number of cycles, horizontal arrows indicate the direction of the potential scan

Table 1. **Conditions for co-polymer preparation**

Monomers	*c*, mM	No. of CV cycles	Supporting electrolyte composition	*E* interval, V	*v*, mV/s	Obtained co-polymer
FA : Rf	1.00 : 3.00	32	0.1 M PBS pH 6.0	−1.00 V – +1.50	50	PFA-PRf3
FA : Rf	1.00 : 5.00	32	0.1 M PBS pH 6.0	−1.00 V – +1.50	50	PFA-PRf5
FA : Rf	1.00 : 10.0	32	0.1 M PBS pH 6.0	−1.00 V – +1.50	50	PFA-PRf10
FA : LL	0.100 : 1.00	20	0.1 M PBS pH 5.5 + 0.1 M K_2SO_4	−1.00 V – +2.20	50	PFA-PLL

Furthermore, the current densities were lower during the co-polymer formation than those of separate polymers.

None of the obtained co-polymers was stable, they were washed out from the surface during the repeated potential cycling in the buffer solution at neutral pH. Therefore, another approach was used to obtain different co-polymer based on the previous experience with the polymerisation of amino acid L-lysine [27]. FA was chosen as a co-monomer to LL to ensure better sensitivity of the modified electrode to analyte. The polymerisation CVs are given in Fig. 3. CV profile is different from that of FA (Fig. 2a), but more similar to LL polymerisation (not shown, was presented in Ref. [27]) with exception of a clear oxidation peak at +1.52 V, where FA overoxidized. Like in other co-polymer cases, the current density is increasing with the number of potential cycles until a steady-state is reached. Further cycling causes a decrease in the current density which means either film decomposition due to overoxidation or changes in the film structure. This film was stable even after multiple potential cycling in a buffer solution. This film was further applied for atrazine detection.

Co-polymer film topography was characterised using AFM and the obtained images are depicted in Fig. 4. In both cases of PFA-PRf5 and PFA-PRf10, a thin continuous film was observed with randomly spread nanostructures. The nanoparticles were larger in width and height in the PFA-PRf5 [28]. The highest structures were 1.25 nm in height and 10–20 nm in width (Fig. 4a). Since in some places holes are observed, which means that gas bubbles were appearing during the polymerisation process and most probably it was oxygen during the overoxidation process. Similar heights of the nanoparticles were also observed in the co-polymer PFA-PRf10. Only in this case, larger HOPG terraces were visible. However, in this case, the nanoparticles were from 1 to 5 nm (Fig. 4b).

A similar view was obtained also for PLL/HOPG, which was published previously [27]. The difference is only that the nanoclusters of the polymer were condensed along the step defects of HOPG terraces.

The electrochemical characterisation was performed using CV at PFA-PRf5 and PFA-PRf10 with an addition of a redox probe because without it the co-polymer peaks were not well defined. First, CV was used for characterisation at different potential scan rates (Fig. 5).

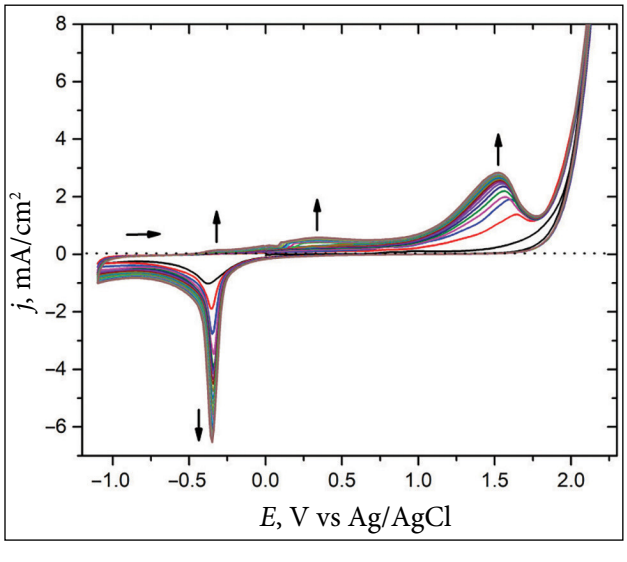

Fig. 3. CVs for FA-LL electropolymerisation at GCE in 0.1 M PBS with 0.1 M K_2SO_4, pH 5.5, monomer ratio was 0.1:1 mM. The potential interval was between −1.10 V and +2.20 V, 20 cycles, potential scan rate 50 mV/s. The meaning of the arrows is the same as in Fig. 1

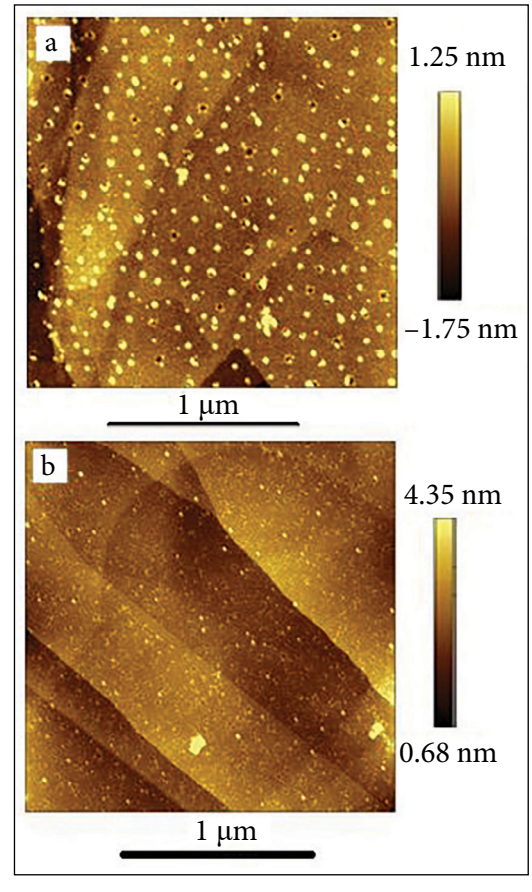

Fig. 4. AFM images of PFA-PRf deposited on HOPG at pH 6.0. Monomer ratio 1:5 (a) and 1:10 (b)

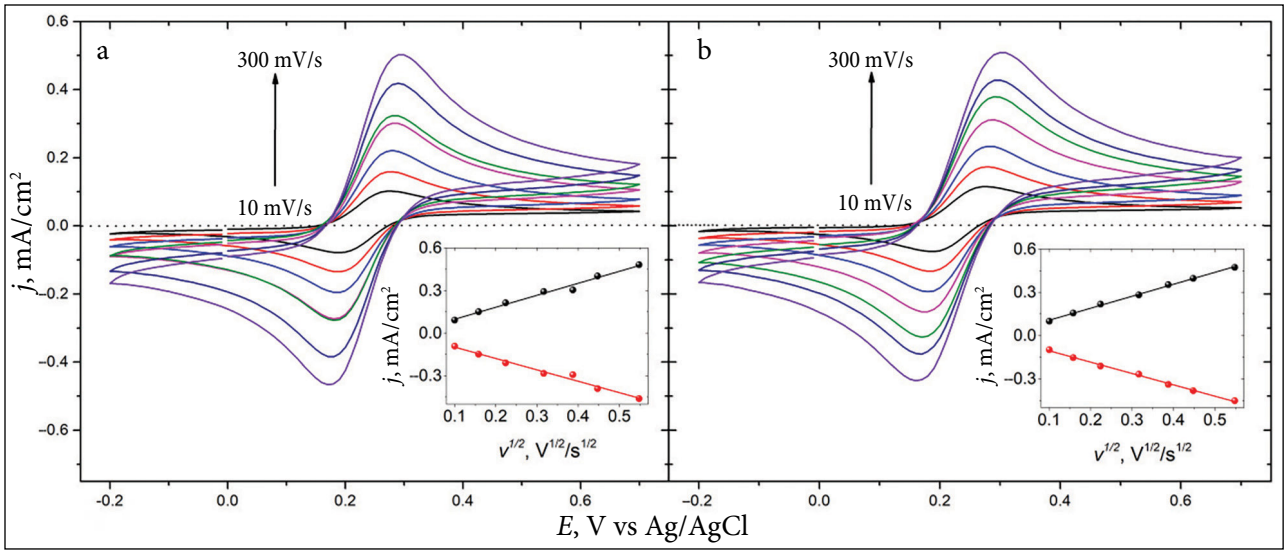

Fig. 5. CVs at PFA-PRf5/GCE (a) and PFA-PRf10/GCE (b) in the 0.1 M KCl/HCl solution with addition of 2.0 mM $K_4[Fe(CN)_6]$ at different scan rates (10, 25, 50, 100, 150, 200 and 300 mV s^{-1}) after background subtraction. Insets show the dependence of peak current density on the square root of the potential scan rate

As seen, the CV profile was actually the same at both co-polymer-modified electrodes (Fig. 5). In both cases, the peak difference was 90 mV indicating a quasi-reversible process, which was caused by different electrode kinetics at the co-polymer than that at the bare electrode [29]. In both cases, the electrochemical process was diffusion-limited since peak current density depends on the square root of the potential scan rate (Fig. 5, insets). The slopes were 0.835 ± 0.033 and –0.795 ± 0.034 mA cm^{-2} $mV^{1/2}$ $s^{-1/2}$ for oxidation and reduction, respectively. The electroactive area (A_{EA}) calculated using the Randles–Ševčik equation was 0.043 cm^2 for both electrodes. The geometric area was larger (0.071 cm^2) as is usual in the case of B vitamin-based polymers without other modifications [28].

Then PFA-PLL/GCE was characterised under the same conditions. As seen in Fig. 6, the peak-to-peak difference is even higher and it was 140 mV, indicating an irreversible electron transfer process. Due to this reason, it was not possible to determine A_{EA} using the Randles–Ševčik equation. Moreover, the oxidation and reduction processes undergo different mechanisms because the linear dependence on the square root of the potential scan rate was only for oxidation (the slope 1.61 ± 0.10 mA cm^{-2} $mV^{1/2}$ $s^{-1/2}$), while reduction peak current density depended on the scan rate with the slope 4.49 ± 0.14 mA cm^{-2} mV s^{-1} (not shown) indicating adsorption limited process.

A_{EA} was calculated from the adsorption process using the double-layer capacitance method [30]

$$A_{EA} = C_{dl}/C_s, \quad (1)$$

where C_{dl} (in mF) is the double-layer capacitance and C_s (in mF cm^{-2}) is the specific capacitance. C_{dl} is equal to

$$C_{dl} = I/v, \quad (2)$$

i.e. the current dependence on the potential scan rate in the double-layer region. Consequently, A_{EA}

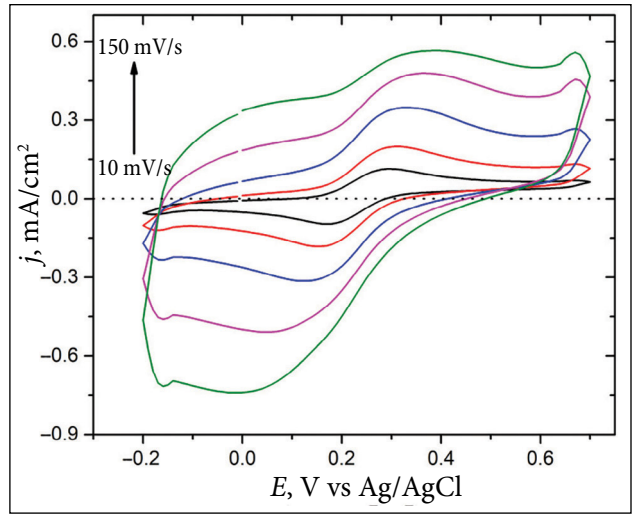

Fig. 6. CVs at PFA-PLL/GCE in 0.1 M KCl/HCl solution with addition of 2.0 mM $K_4[Fe(CN)_6]$ at different scan rates (10, 25, 50, 100, 150, 200 and 300 mV s^{-1}) after background subtraction

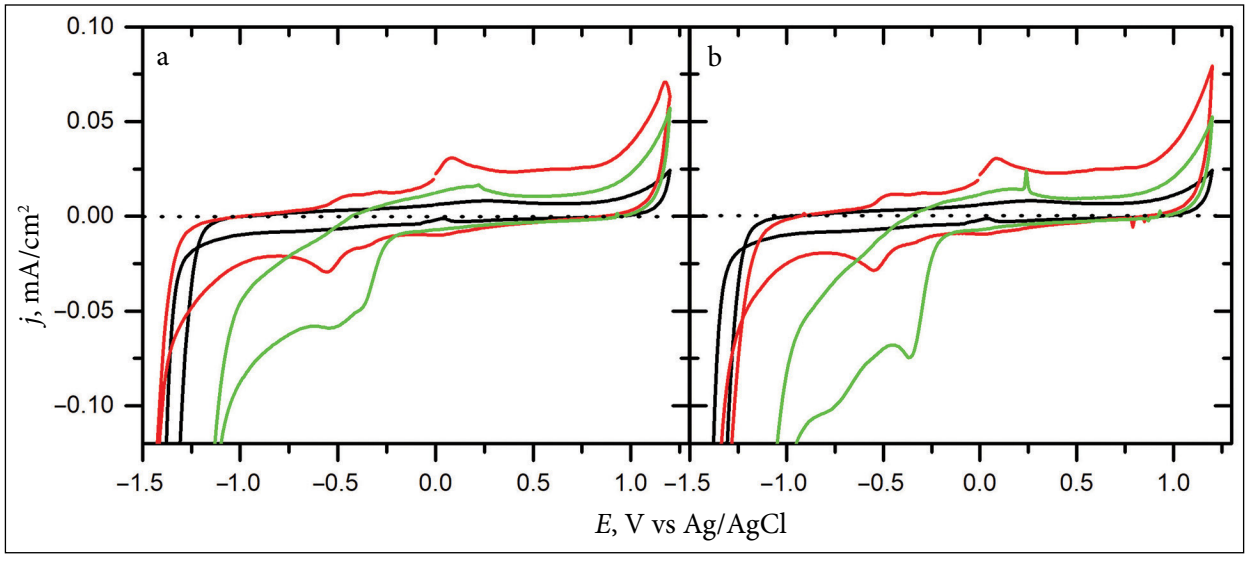

Fig. 7. CVs at PFA-PRf5/GCE (a) and PFA-PRf10/GCE (b) in 0.1 M PBS, pH 5.0, potential scan rate was 50 mV/s. The black line indicates bare GCE, the red line PFA-PRF/GCE, and the green line co-polymer modified electrode with 21.9 μM atrazine

was 0.025 cm², which again is lower than the geometric area (0.071 cm²).

The PFA-PRf co-polymer modified electrode was applied for the investigation of response to atrazine. As seen in Fig. 7, atrazine has a great impact on the reduction current density, and the co-polymer peaks were shifted towards less negative potential values. The response to 21.9 μM of atrazine was 35.0 and 41.1 μA/cm² at PFA-PRf5/GCE and PFA-PRf10/GCE, respectively. Although the response to atrazine was promising, however, due to the instability of the co-polymer films, it was irreproducible.

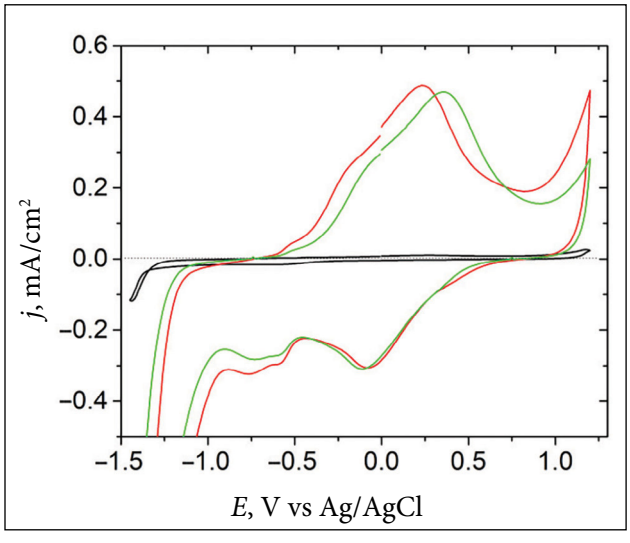

Fig. 8. CVs at bare GCE (black line) and PFA-PLL/GCE without (red line) and with 21.9 μM of atrazine (green line) in 0.1 M PBS, pH 5.0 at a scan rate of 50 mV/s

Different response to atrazine was observed at PFA-PLL/GCE using CV (Fig. 8). At this co-polymer, the current density was a magnitude higher although the FA concentration was 10 times lower than that at PFA-PRf/GCE (Table 1). In this case, the atrazine addition caused an increase in the current density which was well expressed in both cathodic and anodic regions where PFA reduction or oxidation, respectively, occurs. The cathodic response was 42.0 μA/cm², while the anodic response was ca. 13.1 μA/cm² to 21.9 μM of atrazine. This signal, differently from PFA-PRf, was more reproducible than that at PFA-PRf/GCE.

Usually, CV is not the most sensitive method for analyte detection, and, therefore, SWV and chronoamperometry were used as well to investigate the response to atrazine. SWVs at PFA-PLL/GCE are depicted in Fig. 9a. The subsequent addition from 400 nM to 22 μM resulted in an increase of current density in the whole potential region studied being the clearest at the peak position of PFA oxidation, i.e. −1.12 V and, a new oxidation wave appeared at −0.650 V.

The final reaction of atrazine oxidation is shown in Eq. (3) [31],

$$C_8H_{14}ClN_5 + 31H_2O \rightarrow 8CO_2 + Cl^- + 5NO_3^- + 76H^+ + 70e^-, \quad (3)$$

but the first step, which is observed in SWV, is its oxidation to cyanouric acid [31].

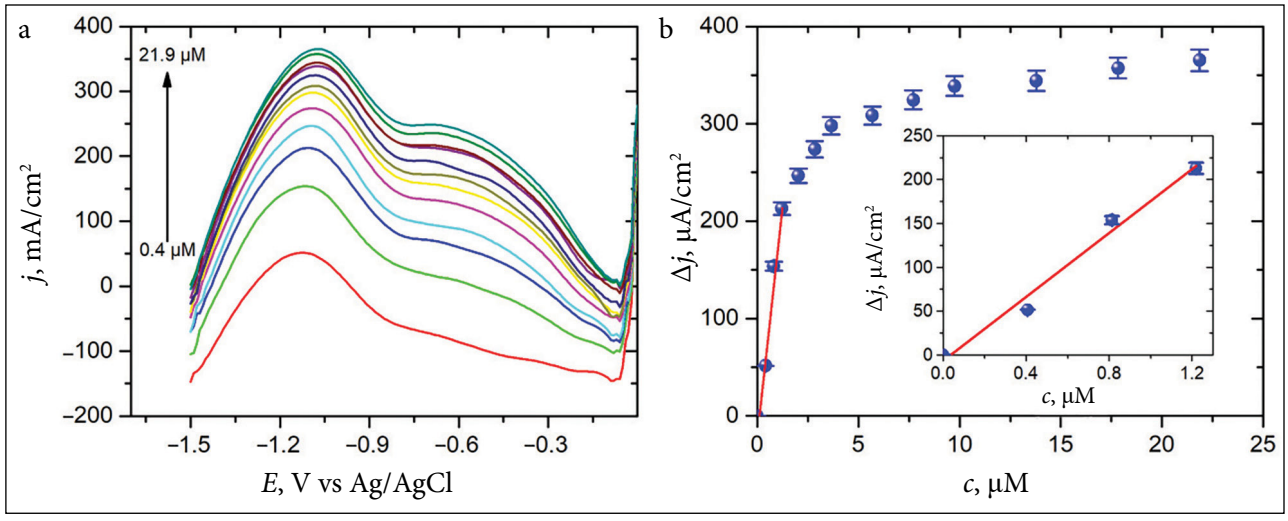

Fig. 9. SWVs at PFA-PLL/GCE (a). The potential amplitude was 10 mV with a frequency of 50 Hz. Other conditions as in Fig. 8. Atrazine additions were 0.400, 0.800, 1.20, 2.00, 2.90, 3.70, 5.70, 7.70, 9.70, 13.8, 17.8 and 21.9 μM. A calibration curve of atrazine at the same electrode (b) was calculated from data in (a)

As the calibration curve in Fig. 9b shows, the process has 2 linear ranges, the first one is short but with a high sensitivity of 198 ± 1 μA/μM cm², and the limit of detection (LOD) obtained using the 3σ method was 14.8 nM.

Voltammetries are also less convenient methods in practical applications while fixed potential ones are more suitable. Therefore, chronoamperometry was also performed to evaluate the response signal to atrazine. Figure 10 depicts a chronoamperogram obtained at the same electrode under the same conditions as in Fig. 8, while the potential was fixed at –0.60 V, where the best response in CV and SWV was obtained, on the one hand. And, on the other hand, it has been optimised by measuring the response signals at various potentials from –0.400 to –0.900 V (Table 2). Although the best signal was at –0.900 (–376 nA), it is not suitable for practical applications due to high interferences because at this potential many substances are reduced including hydrogen evolution. Therefore, the potential was fixed at –0.600 V as it had the first sufficiently high response (–176 nA).

As seen from Fig. 10, each addition of atrazine caused a decrease in the cathodic current, but the response time was rather slow, ca. 1 min. The sensitivity was 8.39 ± 0.39 μA/μM cm^{-2}, in this case, much lower than that at SWV. LOD was

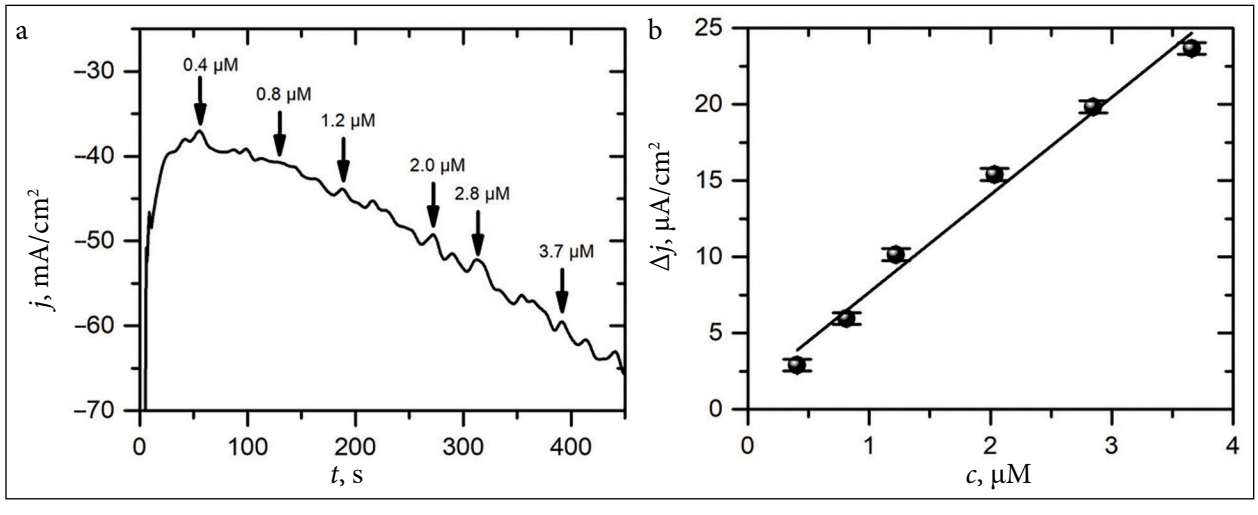

Fig. 10. Part of the fixed potential chronoamperogram at PFA-PLL/GCE at –0.6 V. The black arrows show additions of atrazine. Other conditions as in Fig. 8. PFA-PLL/GCE calibration curve (b) obtained from the chronoamperogram in (a)

Table 2. **Optimisation of potential for atrazine detection using fixed potential chronoamperometry**

E, V	*I*, nA
–0.400	–110
–0.500	–116
–0.600	–176
–0.700	–174
–0.800	–351
–0.900	–376

also lower 10 times and equal to 139 nM. This means that the fixed potential process at the optimised process was not suitable for the analysis under real conditions.

The obtained sensor was tested for atrazine detection in tap water, which was diluted with phosphate buffer to keep the constant pH. Since atrazine is not present in tap water, it was added to the sample solution. When the aliquots of atrazine were added, SWV was registered after each addition. The response in tap water samples was significantly higher than that in the pure buffer solution, moreover, the linear range was also shorter (not shown). Therefore, to determine atrazine in ground- or waste-water the spiking method is most suitable when calibration is made in the sample directly because a sample nature (pH was kept the same as in buffer solution) has an impact on both the background and response signals. The sensitivity to atrazine in tap water was 74.6 ± 4.4 μA/μM cm^2, which is lower than in PBS only, but it is still much better than using chronoamperometry.

CONCLUSIONS

Electrochemically co-polymerised FA and Rf with three different ratios (1:3, 1:5, 1:10) of the monomers as well as FA and LL (1:10) were used for the detection of atrazine using votammetries and chronoamperometry. The microscopic investigation showed that in all cases co-polymers form nanoparticles which means that polymerisation starts at some polymerisation centres on the surface defects. The electrochemical characterisation revealed that the electrochemical process is diffusion limited. However, all PFA-PRf films were unstable and were washed out from the electrode surface. The optimal composition of the sensor was PFA-PLL/GCE when the ratio of monomers was 1:10. This sensor gave the best stability and sensitivity to atrazine. The best sensitivity to atrazine was 198 ± 1 μA/μM cm^2, and the LOD was 14.8 nM. However, the sensitivity in tap water was significantly lower (74.6 ± 4.4 μA/μM cm^2) but still suitable for atrazine detection using the spike method.

Received 27 October 2022
Accepted 31 October 2022

ACKNOWLEDGEMENTS

The work is devoted to the anniversary of Prof. Rimantas Ramanauskas.

References

1. *World Health Organization* [https://www.who.int/news-room/questions-and-answers/item/chemical-safety-pesticides].
2. *US Environmental Protection Agency* [https://www.epa.gov/ingredients-used-pesticide-products/atrazine].
3. T. R. Steinheimer, M. G. Ondrus, *Water-Resources Investigations Report 89–4193*, U.S. Geological Survey (1990).
4. R. A. Yokley, M. W. Cheung, *J. Agric. Food Chem.*, **48**, 4500–4507 (2000).
5. S. B. Huang, J. S. Stanton, Y. Lin, R. A. Yokley, *J. Agric. Food Chem.*, **51**, 7252–7258 (2003).
6. I. Baranowska, H. Barchanska, R. A. Abuknesha, R. G. Price, A. Stalmach, *Ecotoxicol. Environ. Safety*, **70**, 341–348 (2008).
7. J. A. A. Pascua, A. J. A. Prado, B. R. B. Solis, A. P. Cid-Andres, C. J. B. Cambiador, *Spectrochim. Acta A*, **220**, 116837 (2019).
8. J. Shah, M. R. Jan, B. Ara, *Environ. Chem. Lett.*, **8**, 253–259 (2010).
9. M. Muhammad, J. Shah, M. R. Jan, B. Ara, M. M. Khan, A. Jan, *Anal. Sci.*, **32**, 313–316 (2016).
10. C. Saha, M. Bhushan, L. R. Singh, *J. Iran Chem. Soc.* (2022).
11. R. W. Keay, C. J. McNeil, *Biosens. Bioelectron.*, **13**, 963–70 (1998).
12. K. Grennan, G. Strachan, A. J. Porter, A. J. Killard, M. R. Smyth, *Anal. Chim. Acta*, **500**, 287–298 (2003).
13. E. Zacco, R. Galve, F. S. Baeza, M. P. Marco, S. Alegret, M. I. Pividori, *Comprehens. Anal. Chem.*, **49**, e233–e236 (2007).
14. P. Norouzi, B. Larijani, M. R. Ganjali, F. Faridbod, *Int. J. Electrochem. Sci.*, **7**, 10414–10426 (2012).
15. L. Švorc, M. Rievaj, D. Bustin, *Sens. Actuat. B*, **181**, 294–300 (2013).

16. K. Calfumán, J. Honores, M. Isaacs, D. Quezada, J. Valdebenito, M. Urzúa, *Electroanalysis*, **31**, 671–677 (2019).
17. P. Supraj, S. Tripathy, S. R. K. Vanjari, V. Singh, S. G. Singh, *Biosens. Bioelectron*., **141**, 111441 (2019).
18. P. Supraj, S. Tripathy, S. R. K. Vanjari, V. Singh, S. G. Singh, *Sens. Actuat. B*, **285**, 317–325 (2019).
19. N. F. C. Lah, A. L. Ahmad, S. C. Low, N. D. Zaulkiflee, *Membranes*, **11**, 657 (2021).
20. R. Zumpano, M. Manghisi, F. Polli et al., *Anal. Bioanal. Chem.*, **414**, 2055–2064 (2022).
21. N. Shoaie, M. Daneshpour, M. Azimzadeh, et al., *Microchim. Acta*, **186**, 465 (2019).
22. E. Pardieu, H. Cheap, C. Vedrine, et al., *Anal. Chim. Acta*, **649**, 236–45 (2009).
23. N. V. Chuc, N. H. Binh, C. T. Thanh, et al., *J. Mater. Sci. Technol*., **6**, 539–544 (2016).
24. T. Venckus, R. Celiešiūtė, A. Radzevič, et al., *Electroanalysis*, **26**, 2273–2282 (2014).
25. R. Celiešiūtė, A. Radzevič, A. Žukauskas, Š. Vaitekonis, R. Pauliukaite, *Electroanalysis*, **29**, 1–13 (2017).
26. V. Žutautas, T. Jelinskas, R. Pauliukaite, *J. Electroanal. Chem*., **921**, 116668 (2022).
27. L. Laurinavičius, A. Radzevič, I. Ignatjev, et al., *Electrochim. Acta*, **299**, 936–945 (2019).
28. A. Radzevič, Master Thesis, Vilnius University, Vilnius (2016).
29. D. Guziejewski, L. Stojanov, R. Gulaboski, V. Mirceski, *J. Phys. Chem. C*, **126**, 5584–5591 (2022).
30. P. Zhu, Y. Zhao, *RSC Adv*., **7**, 26392–26400 (2017).
31. N. Borràs, R. Oliver, C. Arias, E. Brillas, *J. Phys. Chem. A*, **114**, 6613–6621 (2010).

Emilija Katinaitė, Vytautas Žutautas, Aneta Bytautaitė, Rasa Pauliukaitė

NAUJA ELEKTROCHEMINIO JUTIKLIO ATRAZINUI APTIKTI SUKŪRIMO STRATEGIJA

S a n t r a u k a

Pesticidų nustatymas yra ypač svarbus žmonių sveikatai. Vienas šios problemos sprendimo būdų yra jutikliai, nes juos galima naudoti ne tik laboratorinėmis sąlygomis. Elektrocheminiai jutikliai yra lengvai miniatiūrizuojami ir taikomi pesticidams nustatyti tiek gruntiniuose vandenyse, tiek nuotekose. Laidūs polimerai elektrocheminiuose jutikliuose atlieka kelis vaidmenis, todėl yra tinkami ir jutiklių, skirtų pesticidams aptikti, kūrimui. Elektrochemiškai kopolimerinti folio rūgštis ir riboflavinas bei folio rūgštis ir L-lizinas buvo taikomi pesticido atrazino nustatymui kvadratinės bangos voltamperometrijos (KBV) metodu. Kopolimerų sudėtis buvo optimizuota tiriant juos mikroskopiškai ir elektrochemiškai. Tinkamiausia sudėtis pagal jautrį atrazinui buvo polifolio rūgšties ir poli-L-lizino kopolimeras, kur monomerų santykis buvo 1:10. Tinkamiausias metodas buvo KBV, kurio jautris atrazinui buvo 198 ± 1 μA/μM cm^2, o nustatymo riba 14,8 nM. Deja, čiaupo vandenyje jautris gerokai sumažėjo, bet jutiklis vis dar tinkamas praktiniams tyrimams, naudojant standartinių priedų metodą.